PSFC/JA-01-17

OBSERVATION OF MULTIPLE CASCADE STEPS OF THE LANGMUIR DECAY INSTABILITY IN A LASER PLASMA

R. J. Focia,[1] D. S. Montgomery,[2]
J. C. Fernández,[2] and R. P. Johnson[2]

[1]Plasma Science & Fusion Center
Massachusetts Institute of Technology
Cambridge, Massachusetts 02139 USA

[2]Los Alamos National Laboratory
Los Alamos, New Mexico 87545 USA

July 2001

This work was supported by the Los Alamos National Laboratory Contract No. E29060017-8F. Reproduction, translation, publication, use and disposal, in whole or part, by or for the United States Government is permitted.

To appear in *Physical Review Letters*.

Observation of Multiple Cascade Steps of the Langmuir Decay Instability in a Laser Plasma

R.J. Focia, D.S. Montgomery[1], J.C. Fernández[1], and R.P. Johnson[1]
Plasma Science and Fusion Center, Massachusetts Institute of Technology, Cambridge, Massachusetts 02139
[1]*Los Alamos National Laboratory, Los Alamos, New Mexico 87545*

Stimulated Raman scattering (SRS) can be non-linearly coupled to other parametric instabilities, such as the Langmuir decay instability in which an electron plasma wave (EPW) decays into a counterpropagating EPW and a copropagating ion acoustic wave. This process can result in a cascade of counter and copropagating EPWs. We have unambigously observed this cascade using collective Thomson scattering. For the conditions of the study we observed two cascade steps. The Thomson spectra is well correlated with measurements of the backscattered SRS light as expected since SRS drives the process.

PACS Codes: 52.35.Fp, 52.35.Mw, 52.70.Kz

Preprint - Submitted to the PRL 5/15/01

Control of parametric laser-plasma interactions is essential to the success of inertial confinement fusion (ICF) [1]. Stimulated Raman scattering (SRS) is one such interaction involving the resonant decay of an incident electromagnetic wave (EMW) into a scattered EMW and an electron plasma (or Langmuir) wave (EPW). SRS is undesirable not only because it can cause losses in drive energy and illumination symmetry but also because it can trap and accelerate electrons that could preheat the fusion capsule. The onset and scaling of SRS has been the subject of much investigation [2].

In quasi-homogeneous ignition-relevant plasmas, the EPW amplitude can be large for moderate SRS reflectivity so that saturation by nonlinear mechanisms is expected and

observed [3,4]. One possible source of non-linearity is coupling of SRS to other parametric processes via wave-wave interactions. One such mechanism is the Langmuir decay instability (LDI) [5], where the daughter EPW from SRS decays into an EPW and an ion acoustic wave (IAW). LDI occurs when the amplitude of the primary EPW exceeds a threshold that is proportional to the product of the damping rates for the secondary EPW and IAW. The growth rate for LDI is maximized when the daughter EPW and IAW are propagating antiparallel and parallel, respectively, to the primary EPW. Subsequent EPW decays due to LDI are possible if their amplitudes exceed the threshold. In this Letter we use the terminology that an EPW generated by LDI is called an LDI cascade step and, collectively, more than one cascade step is called LDI cascade. The LDI cascade can saturate SRS since wave energy from the SRS EPW couples into secondary EPWs and IAWs that are non-resonant with the SRS process. The saturation effect is strongest when the daughter waves are strongly damped. Backward propagating EPWs presumed to be from LDI have been observed [6] and LDI has been observed in ionospheric plasmas [7]. Observation of Langmuir turbulence in a laser-produced plasma has been reported recently [8]. However, it could not be established whether strong turbulence or weak LDI cascade was observed in those experiments due to inhomogeneity [9].

In this Letter, we present the first unambiguous observations of multiple LDI cascade steps driven by SRS backscatter. The experiment was conducted at the Los Alamos National Laboratory (LANL) using the TRIDENT laser facility [10]. In the experiment, a preformed plasma is illuminated with a nearly diffraction-limited single hot spot (SHS) laser [11] to drive SRS in a plasma. The SHS laser focal spot is characterized by a speckle width of $F\lambda_0 \approx 2.5 \pm 0.15$ μm and speckle length of $7F^2\lambda_0 \approx 75$μm, where λ_0 is the laser wavelength (527

nm for the SHS interaction laser) and F is the focal ratio of the focusing optic. The plasma initial conditions are homogeneous on the scale of the laser focal spot volume where the interaction occurs, and enables the observation of fine spectral structure associated with LDI cascade. This removes any ambiguity due to inhomogeneity when interpreting the data. The initial conditions of these plasmas have been thoroughly characterized elsewhere [11]. The conditions for our experiment were also monitored as described below. The EPW spectrum from SRS and LDI is measured using collective Thomson scattering, and structure is observed in the spectra consistent with LDI cascade. Up to two LDI cascade steps are inferred from the measurements presented here.

A schematic of the experimental setup is shown in Fig. 1. The plasma is formed by vaporizing a thin foil target and heating it with a line-focused λ=527 nm laser beam. This heater beam is defocused so as to create a plasma with density scale lengths transverse and parallel to the interaction laser focal spot of ~200 μm and ~1000 μm, respectively. Thus, the plasma is considered quasi-homogeneous over the interaction volume of the SHS. The targets used were ~1 mm in diameter and ~6.5 μm thick parylene (C_8H_8). The heater beam has a flat-topped pulse profile with duration of 1.2 ns full-width at half maximum (FWHM). At a time 200 ps after the heater beam is turned off the interaction beam (λ=527 nm), having a Gaussian pulse width of 200$\pm$10 ps FWHM, is focused into the plasma through an f/4.4 lens perpendicular to the plasma flow (i.e. parallel to the original surface of the target). The location of the SHS was ~400 μm in front of the target, resulting in $n_e/n_c \approx$3.1-3.2% as inferred from the backscattered SRS data shown later. Here, n_e is the electron density and n_c ($\approx 4 \times 10^{21}$ cm^{-3}) is the critical density above which light does not propagate. The ultraviolet (λ=351 nm) Thomson probe beam is also a Gaussian pulse with a 200$\pm$10 ps FWHM,

coincident in time with the interaction beam, and is focused into the plasma through an f/4.5 lens. The Thomson scattered light is collected through the full aperture of the collection optic (f/4). The Thomson scattering diagnostic was set up to look only at the forward propagating EPWs, i.e. those propagating in the same direction as the interaction laser. Although we do not image the backward propagating EPWs their presence is inferred from the resultant Thomson spectrum.

Thomson scattering is a resonant process that requires frequency, ω and wave vector, $\vec{k}$ matching be satisfied [12]. Frequency and wave vector matching cannot be achieved with arbitrary probe and collection angles. To calculate the resonance points and thus the probe and collection angles required, we use the usual dispersion relation for an EM wave in a plasma and kinetic dispersion relations for EPWs and IAWs. The focal ratio of the probe and collection optics allows for a finite range of wave vectors (and frequencies for the scattered light) to participate in the Thomson scattering. The Thomson probe was set up to investigate plasma densities near $n_e/n_c \approx 3\%$. The probe beam was focussed into the plasma at 50 ± 6.3 degrees and the scattered light was collected at 63 ± 7.1 degrees, which allowed probing waves parallel to k_o (the free space wave number of the SHS beam) from $1.34k_o$ to $1.76k_o$. We calculate that our diagnostic would allow resolution of the SRS EPW and up to three subsequent forward-propagating LDI cascade steps. Half of the Thomson scattered light was sent to a time-resolved diagnostic that integrated over the scattered wave vectors, and the other half was sent to a diagnostic that resolved the wavelength versus angle on the collection optic (effectively ω vs. $\vec{k}$) and was time-integrated over the duration of the probe pulse. The latter was accomplished by imaging the optic plane of the collection lens, rather than its focal plane [13]. This diagnostic was useful for obtaining the dispersion properties of

the LDI cascades, and in understanding any structure observed in the time-resolved (wave-vector integrated) Thomson spectra.

The backscattered SRS spectrum from a typical shot in a regime where LDI cascade was observed is shown in Fig. 2. For our present discussion, λ represents the free space wavelength of the measured scattered light, i.e. $\lambda=2\pi c/\omega$, where c is the speed of light. For this shot the laser peak intensity was $I\approx1.92\times10^{15}$ W/cm^2 and the measured SRS reflectivity was R≈3.2%. Thomson scattering from thermal levels of ion acoustic waves from similar shots indicated an initial electron temperature of $T_e\approx350\pm50$ eV, decreasing to ~230±50 eV over the duration of the probe pulse. The SRS spectrum starts at ~659 nm has an intensity weighted centroid of ~657 nm Using the measured SRS wavelengths and T_e, we estimate $k_L\lambda_D\approx0.27$, where k_L is the wavenumber of the SRS Langmuir wave, and λ_D is the electron Debye length.

A rough estimate of the Langmuir wave density fluctuation can be obtained from the SRS reflectivity, and compared to estimates of the LDI threshold as a consistency check [4, 14]. We calculate $(\delta n/n)=[4R_{\max}\Delta k/(n/n_{co})^2k_o^2L]^{1/2}=0.021$ is sufficient to exceed the LDI threshold of $(\delta n/n)_{LDI}=4k_L\lambda_D(\nu_{ia}/\omega_{ia})^{1/2}(\nu_L/\omega_p)^{1/2}=0.018$. In these equations R_{max} is the maximum reflectivity, Δk is the actual spectral width of the SRS (i.e. the observed spectral width corrected for instrument resolution), n is the electron density, k_o and n_{co} are the wave number and critical density of the incident beam, L is the interaction length, (ν_{ia}/ω_{ia}) is the ratio of the IAW damping to its real frequency, and (ν_L/ω_p) is the ratio of the Langmuir wave damping to the plasma frequency. The SRS spectrum clearly shows curvature towards shorter wavelengths over the duration of the laser pulse and there is an

abrupt change in the curvature at time t≈-10 ps. From the SRS spectrum we infer that the plasma density is n_e/n_c~0.032. The decrease in the SRS wavelength with time is accounted for by the measured decrease in T_e. For these conditions the expected separation between the SRS EPW and the first forward propagating EPW from LDI cascade would be ~9.7±0.8 Å.

The time-resolved Thomson spectrum corresponding to the SRS spectrum in Fig. 2 unambiguously shows the signature of LDI cascade (see Fig. 3a). A horizontal lineout of this image where the cascade separation is indicated is shown in Fig. 3b. From the SRS data and an ideal calculation (i.e. using linear theory and resonance matching) we would anticipate the SRS EPW to initially occur at a Thomson wavelength of ~405.1 nm and the observed data is in close agreement. The slight discrepancy in the Thomson wavelength for the SRS EPW (~0.5 nm) is within the uncertainties in the absolute calibration of the SRS and Thomson diagnostic wavelength scales. As indicated in Fig. 3b, the spacing between the SRS EPW and the second cascade is ~10.6 Å and is in excellent agreement with the ideal calculation. The curvature in the Thomson spectrum closely follows that in the SRS spectrum. Although the time axes in Figs. 2 and 3a are not absolutely calibrated with each other, there is an abrupt change in the Thomson spectrum correlated with that in the SRS spectrum. The LDI does not start immediately with the SRS most likely due to being below threshold for the interaction, or due to thermal detuning as indicated by the change in the SRS wavelength with time.

The time-integrated Thomson spectrum corresponding to the SRS and time-resolved Thomson spectra shown in Figs. 2 and 3a, respectively, also shows the signature of LDI cascade (see Fig. 4). Two distinct waves are observed separated in both frequency (Thomson

wavelength) and wave vector (position on the collection optic). The initial spacing in wavelength ($\Delta\lambda \approx 10.6$ Å) and wave vector ($\Delta k/k_o \approx -0.13$) is consistent with the ideal calculation using the density estimated from the SRS spectrum and the early time measurement of T_e. The other characteristics of the spectrum can be modeled using linear theory and resonance matching by assuming a fixed density and a decreasing temperature. The finite focal ratio of the SHS focusing lens allows for a range of wave vectors and frequencies to participate in the SRS interaction. This will result in some fixed initial spread in both ω and k of the SRS EPW. As time progresses T_e and, to a lesser degree, n_e/n_c decrease. The major effect is due to the reduction in the EPW dispersion as a result of the decrease in electron temperature, i.e. thermal flattening. In an underdense plasma, the frequency of the SHS laser and SRS EM waves are much greater than that of the SRS EPW. To satisfy resonance matching as T_e decreases, the change in the SRS EPW wave number will be relatively small. For any subsequent EPWs generated by LDI, a small change in frequency will result in a large change in wave number. For example, assuming a decrease in T_e of 100 eV (from 350 eV), the ideal calculation shows that the relative change in $\Delta\lambda$ and $\Delta k/k_o$ of the second LDI cascade to that of the SRS EPW are 0.94 and 7.1, respectively. Thus, the narrow $\Delta\lambda$, broad $\Delta k/k_o$ time-integrated spectrum is characteristic of an EPW generated by LDI combined with thermal flattening of the EPW dispersion and not some other source of EPWs. The actual change in $\Delta\lambda$ and $\Delta k/k_o$ shown in Fig. 4 do not exactly match the ideal calculation most likely due to uncertainties in the actual T_e in the SHS. However, the qualitative behavior is consistent with linear theory.

Now that LDI cascade is established, a parameter study is necessary to understand the scaling of the number of cascades with plasma parameters and the possible role of LDI

in limiting SRS. A wealth of data was generated from this experiment under various plasma and laser conditions. Presentation of this data is outside the scope of this Letter and will be presented elsewhere in a longer article.

In summary, we have observed multiple LDI cascade steps from the decay of the EPW generated by SRS. The data presented in this Letter shows excellent agreement between the backscattered SRS, time-resolved Thomson, and time-integrated Thomson spectra.

The Authors are indebted to the TRIDENT operations staff in LANL Group P-24 for their hard work, expertise, and dedication, which led to another successful round of experiments. We also thank the Target Fabrication in LANL Group MST-7 for supplying the targets used in the experiment. The lead author is grateful to Prof. A. Bers of MIT for useful discussions and for his efforts in establishing the MIT/LANL research collaboration that allowed participation in the SHS experiments. This work was supported by LANL Contract E29060017-8F.

[1] J. Lindl, Phys. Plasmas **2**, 3933 (1995).

[2] H.A. Baldis, E.M. Campbell, and W.L. Kruer, in *Physics of Laser Plasma*, Handbook of Plasma Physics (North-Holland, Amsterdam, 1991), Vol. 3, Chap. 9.

[3] J.C. Fernández et al., Phys. Rev. Lett. **77**, p. 2702 (1996), Phys. Plasmas **4**, p. 1849 (1997), and Phys. Plasmas **7**, p. 3743 (2000).

[4] R.K. Kirkwood et al., Phys. Rev. Lett. **77**, p. 2706 (1996).

[5] D.F. DuBois and M.V. Goldman, Phys. Rev. Lett. **14**, p. 544 (1965), and Phys. Rev. **164**, p. 207 (1967).

[6] K.S. Baker et al., Phys. Rev. Lett. **77**, p. 67 (1996), and Phys. Plasmas **4**, p. 3012 (1997).

[7] D.F. DuBois, et al., Phys. Plasmas **8**, p. 791 (2001), and P.Y. Cheung et al., Phys. Plasmas **8**, p. 802 (2001).

[8] S. Depierreux et al., Phys. Rev. Lett. **84**, p. 2869 (2000).

[9] D.S. Montgomery, Phys. Rev. Lett. **86**, p. 3686 (2000), and D. Pesme et al., Phys. Rev. Lett. **86**, p. 3687 (2000).

[10] N.K. Moncur et al., App. Opt. **34**, p. 4274 (1995).

[11] D.S. Montgomery et al., Laser and Particle Beams **17**, p. 349 (1999).

[12] J. Sheffield, *Plasma Scattering of Electromagnetic Radiation* (Academic Press, New York, 1975).

[13] D. M. Villeneuve et al., J. Opt. Soc. Am. B **8**, 895 (1991) and D. M. Villeneuve et al., Phys. Rev. Lett. **59**, 1585 (1987).

[14] S. J. Karttunen, Phys. Rev. A **23**, 2006 (1981).

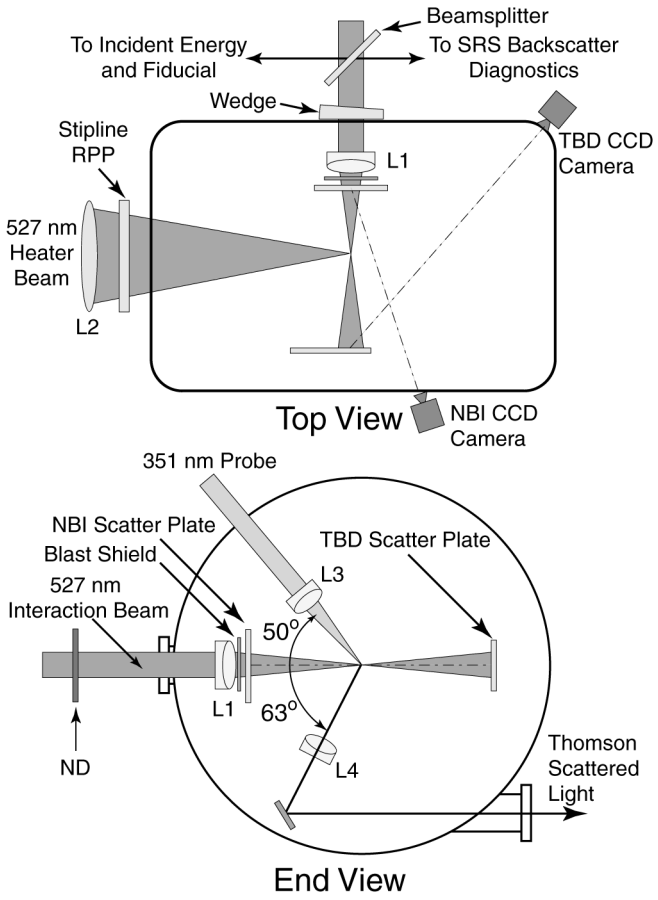

L1: f/4.4 achromat lens
L2: f/6 lens
L3: f/4.5 achromat lens
L4: f/4 achromat lens
ND: Polished ND filters
TBD: Transmitted Beam Diagnostic
NBI: Near Backscatter Imaging

Figure 1. Schematic diagram of the single hot spot experiment.

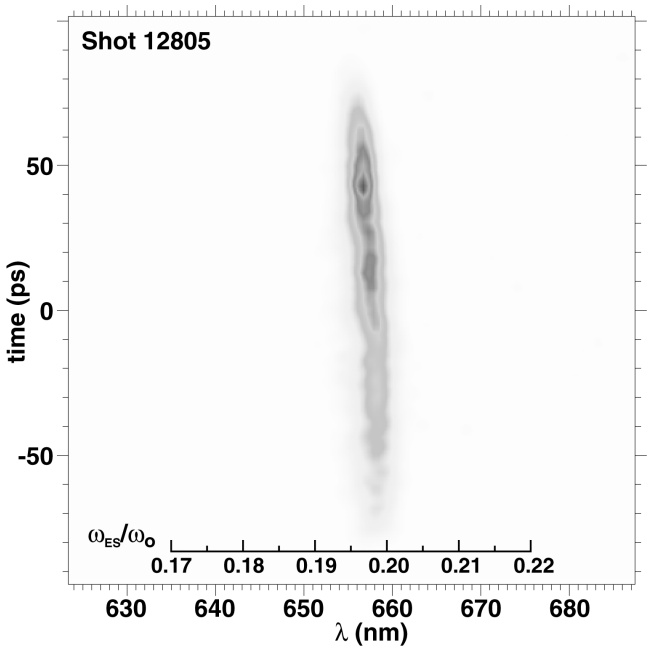

Figure 2. The SRS spectrum observed on shot number 12805. The normalized frequency scale ω_{ES}/ω_o (ω_o is the angular frequency of the SHS laser) shows the expected electrostatic wave frequency for a given wavelength.

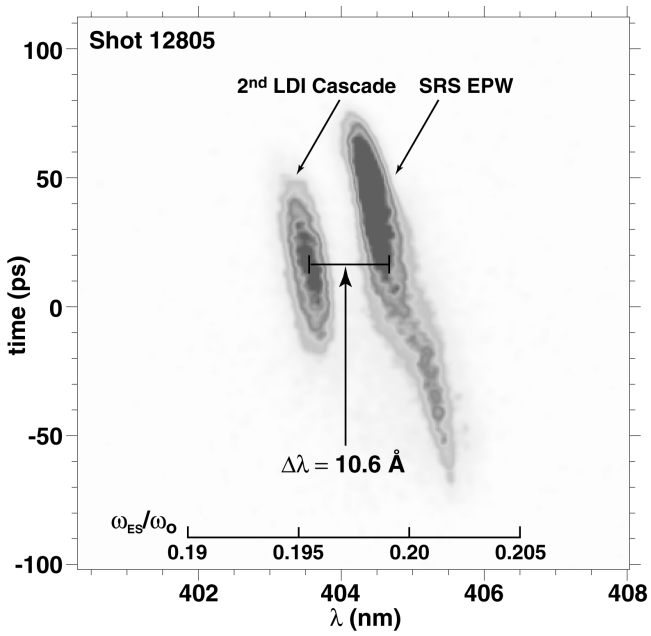

(a)

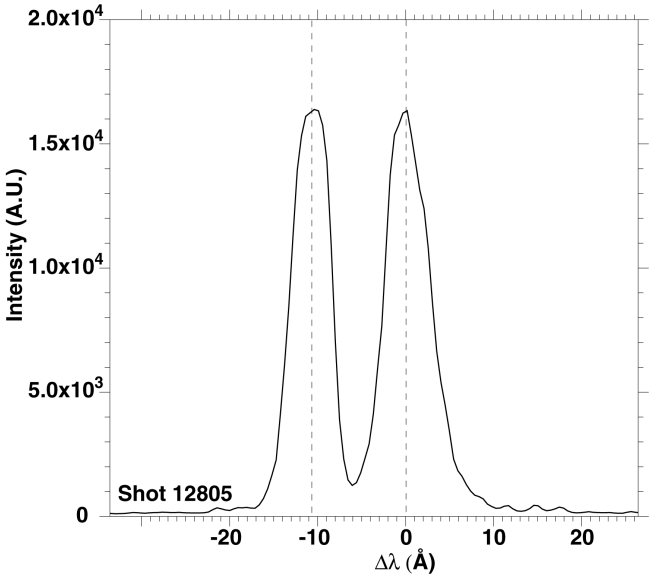

(b)

Figure 3. (a) Time-resolved Thomson spectrum from shot number 12805 showing the forward propagating EPW from SRS and the second LDI cascade. (b) A horizontal lineout taken where the cascade separation is indicated in (a).

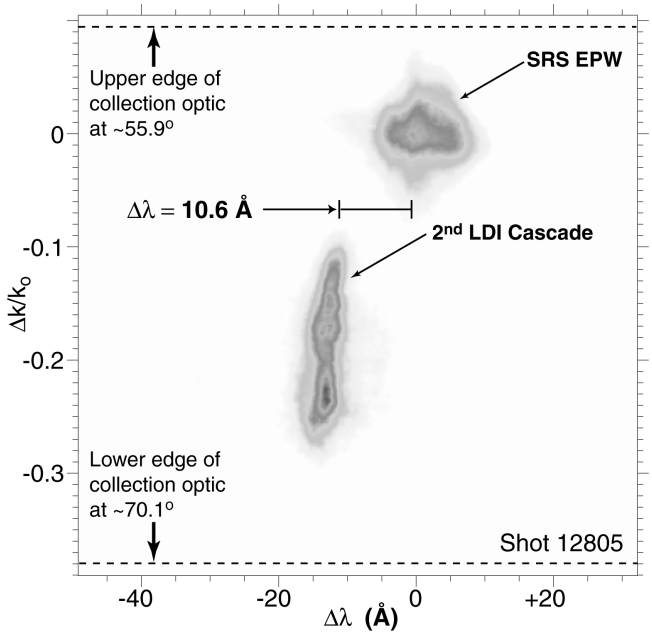

Figure 4. Time-integrated Thomson spectrum from shot number 12805 showing the forward propagating EPW from SRS and the second LDI cascade.